

A Sensor for the Optical Detection of Dangerous Road Condition

Armando Piccardi and Lorenzo Colace

*NooEL - Nonlinear Optics and OptoElectronics Laboratory, Department of Engineering, University of Study "ROMA TRE",
Via Vito Volterra 62, Rome, Italy*

Keywords: Optical Sensor, Light Scattering, Polarization Contrast Ratio.

Abstract: We present the design, realization and characterization of a sensor for the optical detection of hazardous road condition. The device exploits the radiation from a incoherent source to detect the polarized components of the light scattering from a rough surface and calculate a signal dependent on the surface state. We propose two distinct geometries, working with forward and backward scattering components, assessing the device performance in terms of reliability and compactness. In both cases, the sensor allows to discriminate potentially dangerous states like the presence of water (either wet surface or covered by a layer) or ice on an asphalt sample, in opposition to the dry surface representing a safe condition.

1 INTRODUCTION

The automotive sector is currently characterized by a high demand of sensing devices either for the vehicle performances evaluation or the assessment of the drivers safety (Guerrero-Ibáñez, 2018). With reference to the latter, a number of methods and devices have been proposed in the last years in order to detect the presence of atmospheric agents on the road surface. In particular, ice detection rises great attention because of it is not limited to the automotive sector, but it cover a range of possible application ranging from aircraft security to monitoring of surfaces under extreme conditions (Flatscher, 2017; Amiroopoulos, 2018; Muñoz, 2016).

Nevertheless, the trade off between reliability and costs is often a limiting factor for a device thought to meet the market requirements: contact sensors for example, have high maintenance costs though they result quite reliable (Zhi, 2015; Roy, 2000). On the contrary, contact-less devices (Ikiades, 2007) often suffer of poor selectivity to different agents.

The most used methods exploit capacitive, piezoelectric or electrical elements to detect temperature and humidity and evaluate the presence of ice (Wollenweber, 2018; Tabatabai, 2017).

Optical methods and sensors encompass fiber-optics, devices based on infrared image processing light reflection and diffusion at different wavelength ranges (Abdel-Moati, 2018; Finkele, 1997; Ogura,

2002). In particular, light scattering polarization have been recently used to detect the presence of ice or water on asphalt surfaces (Colace, 2013).

In this work, we present the implementation of a device employing an optical method based on the detection of the polarization components of infrared light scattering on asphalt surfaces. Evaluating the ratio between two orthogonally polarized components, we manage to distinguish between several surface conditions and thus between a safe and potentially dangerous states.

The manuscript is organized as follows: first, the optical method, the devices components and the parameters needed to characterize the system are presented. Then, we will describe the realization of different versions of the sensor, changing the geometric arrangement and number of components. The last section is dedicated to the results and the discussion about the system performances.

2 PRINCIPLE OF OPERATION

The proposed sensor works with a light source incident on a sample (asphalt) surface, where the diffusion process changes the distribution of orthogonally (TE and TM) polarized components of the scattered light. In this way, we can obtain information about the surface under investigation depending on the detection of the two polarization components.

In order to implement this method, we need a light source, some detectors and the electronics to process the acquired signals and extract the suitable figures of merit. As done in (Colace, 2013), a useful parameter is the Polarization Contrast Ratio (PCR), defined by the difference between the intensities of the two polarization components (I_{TE} , I_{TM}) normalized by the sum of the two:

$$C = \frac{I_{TE} - I_{TM}}{I_{TE} + I_{TM}} \quad (1)$$

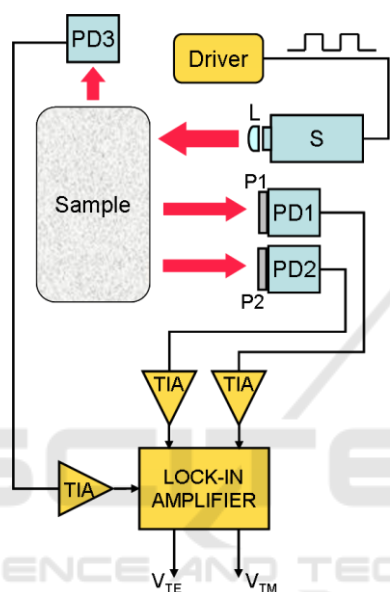


Figure 1: Block diagram of the sensor design. The modulate source (S) emits radiation collimated by a lens (L). The scattered light is detected by the three photodiodes: two (PD1 and PD2) collecting orthogonally polarized light by employing two polarizers (P1 and P2), and the third (PD3) detecting the unpolarized light. Trans impedance amplifiers (TIA) convert the signals to be processed by the lock-in amplifier. The resulting voltage values allow the calculation of the PCR.

Moreover, in our work we also considered the total unpolarized scattering as a parameter to be measured.

The employed source is a LED operating at $\lambda=980\text{nm}$. The chosen wavelength stands in a spectrum range where polarized scattering is rather sensitive to material properties; moreover, near infrared radiation prevents direct disturbance of human eyes while driving and it is compatible with reliable and widely available detection components, in the framework of low cost device realization. A lens is used to compensate for the source diffraction

and to regulate the spot size on the sample in order to optimize the detection.

In order to detect the polarized components and extract the PCR we need two photodetectors, each one sensitive to one component by employing two orthogonal polarizers. The detectors are provided with low pass filters screening any optical disturbances from ambient light. A third photodetector is employed to collect the unpolarized scattering and provide additional formation about the surface.

The reading electronics converts the current signals into voltage signals through distinct trans-impedance amplifiers (TIA) and performs a homodyne detection through a lock-in amplifier. For this reason, the source driver is designed in order to obtain a modulated signal at $f=1\text{kHz}$. The voltage value carrying the information about the polarization components of the scattered light are finally ready to be processed in order to obtain the PCR. We stress that the latter is calculated as in eq.1, but using the voltage values corresponding to the intensities of the polarized components.

The complete set up is sketched in fig. 1.

3 GEOMETRIC ARRANGEMENTS

Given the working principle of the sensor, the components and the quantities needed for the surface detection, we can arrange the set-up in different ways. The sensor works with scattered light, which is distributed over a cone depending on the kind of surface and its roughness as well. For a smooth sample, we expect the incident radiation to be almost reflected forward, while for a rough surface, the light scattering can be supposed isotropic. Thus, the choice of the position where to detect the scattered light can affect the system performances. We investigated two main geometric configurations: the first has the source and the detectors in a $\theta-2\theta$ arrangement, thus detecting the mirror-like polarized reflections; the second works with backscattering, thus detecting the radiation diffused backward and it has the source and the photodiodes arranged in the same position.

The former geometry allow to operate with higher signal levels, but it has higher costs linked to the large area to be dedicated to the sensor. The latter required higher sensitivity as the backscattered signals can be considerably lower but is more convenient in terms of compactness.

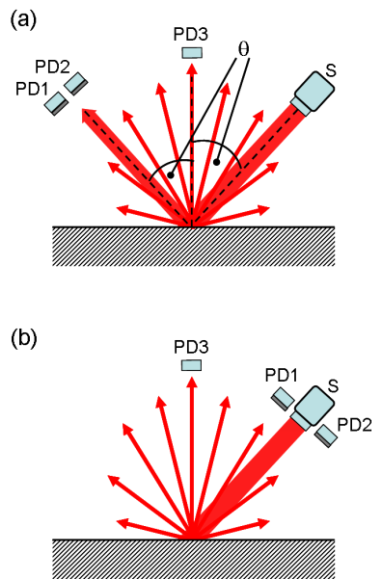


Figure 2: Sketch of the two considered geometries. (a) The mirror-like configuration exploits the Snell law to detect the forward scattered light. (b) The backscattering configuration works with backward diffusion. For both the configurations, a third photodiode can be added to detect the unpolarized scattering.

Moreover, the presence of a third photodetector, collecting the unpolarized scattering to be used as a further measurement to discriminate between different surfaces is evaluated. Its position could be varied as well, but as a reference position we will consider the direction perpendicular to the surface normal.

The geometrical arrangements are resumed in the sketch of fig.2.

4 RESULTS AND DISCUSSION

For both the geometries, the characterization of the sensor is divided into two parts: a preliminary measurements is done by varying the incidence angle of the beam, to check the dependence of the PCR on the source orientation (Videen, 1992). The polarization of the source is varied as well, in order to further improve the system sensitivity to different conditions, exploiting the polarization dependence of the Fresnel coefficients. Then, once optimized the geometry, the detection of the polarization components and the calculation of the suitable parameters are performed on asphalt samples.

In all the presented measurements the source has a power of 18mW and it is at a distance of about 30cm from the surface. We stress that the employed

values can obviously be scaled due to the peculiar application, but at the moment they try to reproduce a possible situation when mounting the device on a moving vehicle or on a road side. Several conditions have been considered. The safe condition is indicated by the values provided by dry asphalt, corresponding to the reference state. Then other surfaces have been prepared corresponding to different atmospheric or road conditions, linked to different level of hazard: wet asphalt, surface covered by a water layer and the presence of an ice layer.

4.1 Mirror-like Configuration

For this configuration the source and the detectors are mounted on a goniometric system ensuring that incidence and detection angle are equal. Incidence angle have been varied between 20° and 60° with respect to the surface normal. Fig. 3 shows the PCR versus incidence angle for some of the surface conditions, when the source radiation is unpolarized or horizontally/vertically polarized.

As it can be seen, both the angle dependence and the absolute value of PCR are strongly dependent on polarization. For unpolarized or horizontally polarized radiation the curves results superposed, for almost all the angular range. On the other hand, vertical polarized light allows the discrimination of different conditions, in particular, between 50° and 60° . Moreover, for 50° the dry asphalt (safe) case has the highest value of PCR, thus it is well distinguishable from the other conditions. For these reasons, we choose $\theta=50^\circ$ to complete the characterization.

At this angle, we calculate the PCR and plot it versus the unpolarized scattering. We performed the measurements a number of times to include the statistical errors of both measurements, also considering several samples for each conditions. Thus, we obtained dispersion graphs on the parameter space for all the road condition, as reported in fig.4. In this way, the separation of the clouds allows finding portions of the parameter space associated to one state, while clouds superpositions indicate the possibility of obtaining a measurement with a certain error percentage.

Fig.4(a) shows a good separation between the states but for the couple dry-ice, for which we calculate an error of about 10%. This represents a problem because the system is interpreting a potentially dangerous condition as a safe one (or *vice versa*). For this reason we checked if it exists another way to represent the different road

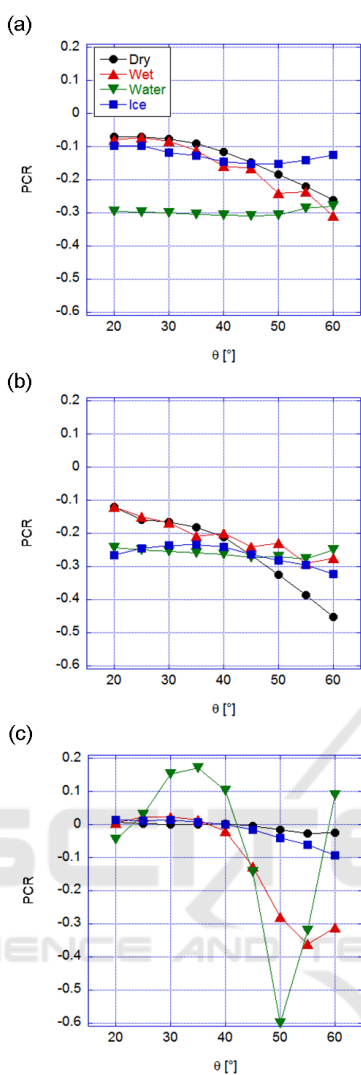


Figure 3: Mirror-like configuration. PCR as a function of the incidence angle for (a) unpolarized, (b) horizontally polarized and (c) vertical polarized incident beam.

conditions: we substitute the unpolarized scattering measurement with the sum of the two polarized components, so that we plot PCR versus sum.

This choice has the further advantage of avoiding the presence of the third photodiode, reducing the complexity and the size of the whole sensor. Results are shown in fig.4(b).

In the new data representation the different states are all distinguishable, allowing a good evaluation of the asphalt conditions. Even if the wet and water cases results close to each other, in practice they correspond to similar hazards and thus their wrong evaluation would have no consequences on the system performances.

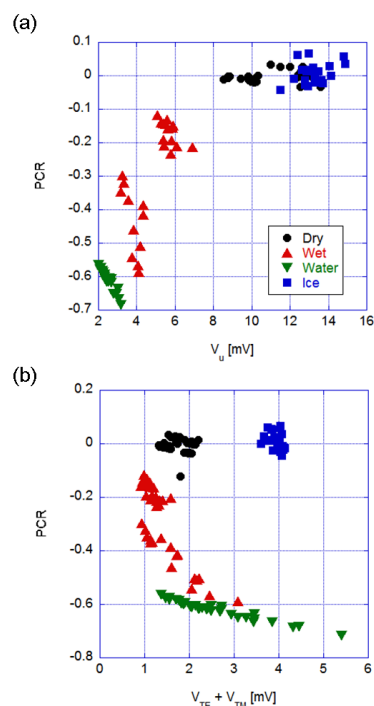


Figure 4: Mirror-like configuration. (a) PCR versus Unpolarized scattering (V_u). (b) PCR versus the sum of the polarization component.

4.2 Backscattering Configuration

The second investigated geometry encompasses source and detectors on the same side, i.e. it detects the backscattering from the asphalt surfaces. We carry out the characterization as for the previous geometry: first, we identify the optimum sensor orientation, by measuring the PCR as a function of the incidence angle for three different polarizations of the source (unpolarized, horizontal and vertical), as reported in fig.5.

This geometry allows a better distinction among the road states than the previous one. Nevertheless, once again the vertical polarization provides the best results; in particular, at $\theta=20^\circ$ the curves are well distributed over a quite range of PCR, thus the complete characterization is performed at this angle.

We plotted the dispersion graphs in both the case with or without the third photodiodes, i.e. considering either the unpolarized scattering or the sum of the orthogonally polarized polarization. In this case, as visible for the direct comparison between panels (a) and (b) of fig.6, differences in the position and distributions of the clouds corresponding to the road states are negligible: this means that the two parameters are equivalent and the

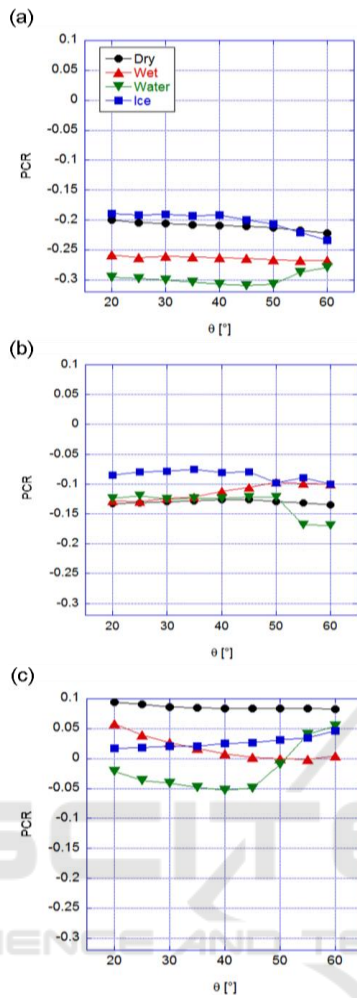


Figure 5: Backscattering radiation. PCR as a function of the incidence angle for (a) unpolarized, (b) horizontally polarized and (c) vertical polarized incident beam.

third photodiode is not necessary at all, thus can be removed with improved sensor compactness and complexity. Moreover, no superposition of clouds is present. Thus, it is straightforward to identify the threshold values and functions for the evaluation of the surface state, as we do in fig.6(b) where we proposed an example of space division based on lines.

With this kind of division the sensor is fully characterized: when the system is working, the measurement of PCR and sum of polarized scattering will generate a point falling into one of the portions of the parameter space. Thus, a programmed logic can be implemented to process the data and give the corresponding indication of the current road state.

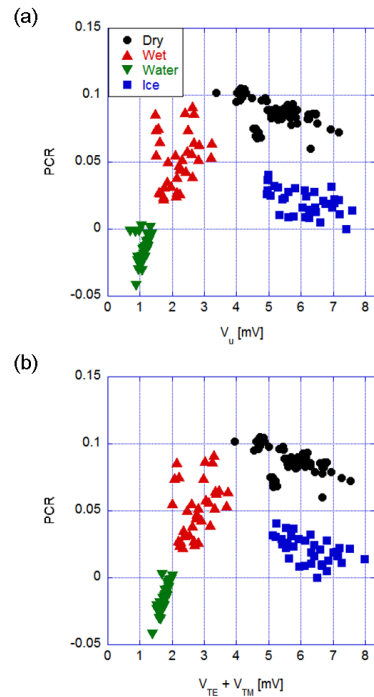


Figure 6: Backscattering configuration. (a) PCR versus Unpolarized scattering (V_u). (b) PCR versus the sum of the polarization component.

5 CONCLUSIONS

We designed, realized and characterized a sensor able to distinguish among for different conditions - one safe and three corresponding to different potentially dangerous situations - of an asphalt surface, in the framework of road security. The optical method used for the detection of a surface state is based on the measurement of the polarization components of the scattered radiation. The investigation of different geometries and configurations allowed to find the optimal set-up in terms of costs and compactness, and to discriminate the presence of water or ice on asphalt surfaces with good reliability. Though in a preliminary version, the realized device and the detection principle are promising and deserve further investigation. Regarding the future developments, the work on the sensor includes the realization of the logic to process the raw data and automatically give information about the surface state and the investigation of other kind of conditions; on the other hand, statistics about the raw data are the object of numerical investigation, in order to improve the detection reliability, as well as a study on the different textures of the investigated surfaces.

ACKNOWLEDGEMENTS

This work was supported by ACTPHAST (Access CenTer for PHotonics InnovAtion Solutions and Technology Support), grant number P2016-29 (SODARC - Sensor for the Optical detection of DAngerous Road Conditions).

REFERENCES

- Abdel-Moati, H., Morris, J., Zeng, Y., Wesley Corie, M., Garas Gianni, V., 2018. Near field ice detection using infrared based optical imaging technology. *Optics & Laser Technology*, 99, 402-410.
- Amiropoulos, K., Spasopoulos, D., Ikiades, A., 2018. Fiber optic sensor for ice detection on aerodynamic surfaces using plastic optic fiber tapers. *Advanced Photonics (Sensors), OSA Technical Digest, SeM4E.6*.
- Colace, L., Santoni, F., Assanto, G., 2013. A near-infrared optoelectronic approach to detection of road conditions. *Optical and Laser Engineering*, 51, 633-636.
- Finkele, R., 1997. Optical road-ice detector operating in the near infrared. *Electronic Letters*, 33, 1153-1154.
- Flatscher, M., Neumayer, M., Bretterkieber, T., 2017. Maintaining critical infrastructure under cold climate conditions: a versatile sensing and heating concept. *Sensors and Actuators A: Physical*, 267, 538-546.
- Guerrero-Ibáñez, J., Zeadally, S., Contreras-Castillo, J., 2018. Sensor Technologies for Intelligent Transportation Systems. *Sensors*, 18, E1212.
- Ikiades, A., Howard, G., Armstrong D.J. et al., 2007. Measurement of optical diffusion properties of ice for direct detection ice accretion sensors. *Sensors and Actuator A*. 140, 24-31.
- Muñoz, C., Márquez, F., Tomás, J., 2016. Ice detection using thermal infrared radiometry on wind turbine blades. *Measurement*, 93, 157-163.
- Ogura, T., Kageyama, I., Katsuhisa N., et al., 2002. Study on a road surface sensing system for snow and ice road. *Journal of Society of Automotive Engineers Review*, 23, 333-339.
- Roy, S., De Anna, R.G., Mehregani, M., Zakar, E., 2000. A capacitive ice detection microsensor. *Sensor Materials*, 12, 1-14.
- Tabatabai, H., Aljuboori, M., 2017. A Novel Concrete-Based Sensor for Detection of Ice and Water on Roads and Bridges. *Sensors*, 17, E2912.
- Videen, G., Hsu, J., Bickel, W.S., Wolfe, W.L., 1992. Polarized light scattered from rough surfaces. *Journal of Optical Society of America*, 7, 1111-1118.
- Wollenweber, G. C., 2018. *US Patent App.*, 15/275, 013.
- Zhi, X., Cho, H.C., Wang, B., Ahn, C.H., Moon, H.S., Go, J.S., 2015. Development of a Capacitive Ice Sensor to Measure Ice Growth in Real Time. *Sensors*, 5, 6688-6698.